cells arrange appropriately in the vestibular sensory epithelia. [74]. Bolstered by further research showing functionality, this study indicates that transplanting neural stem cells may be a promising strategy for replacing damaged HCs. As iterated above, it is logical to use stem cells derived from the same organ that will receive the stem cell transplant. Hence, because the cochlea contains nervous tissue, neural stem cells would be preferential for the treatment of auditory neuropathy and other VIIIth cranial nerve disorders. The use of neural stem cells is also a promising approach for replacing degenerated SGNs. Hu and colleagues report that neural stem cells harvested from adult mice were successfully transplanted into the inner ear of normal and experimentally deafened guinea pigs. They adopted the strategy of biasing the neural stem cells to assume a neuronal phenotype by first transducing them with neurogenin2. Transplanted cells that stained positively for neural class III beta-tubulin were observed close to the sensory epithelium, adjacent to SGNs, suggesting that adult neural stem cells can differentiate into an appropriate phenotype and arrange normally in the inner ear after damage. However, the above-mentioned caveat about functionality also holds here. [75]. These transplantation studies suggest that specific latent cues are present in the adult cochlea that can direct migration and differentiation of experimentally placed neural stem cells.

Finally, it may be possible to genetically engineer adult stem cells to develop into specific cochlear cell types. For instance, a neural stem cell could be developed that conditionally upregulates the Math-1 transcription factor, whose presence has been shown to be sufficient to produce HCs *in vitro* [37] and *in vivo* [52]. With exposure to the appropriate signal, Math-1 would be activated in such a stem cell, destining it to become an HC. Even if the cochlea is devoid of a stem cell source, it may be possible to use stem cells isolated from other tissues as tools for cochlear repair.

4. Conclusions and future directions

Studies on HC regeneration in the avian inner ear have begun to illuminate issues of functional recovery in mammals following HC damage. It has been confirmed that HC regeneration is possible in birds, and the molecular signals that stimulate and inhibit regeneration have begun to be identified. Limited postnatal proliferation and ectopic HC expression has been achieved in mammals by overexpressing Math1, applying cell cycle inhibitors, and transplanting stem cells. These studies may represent the beginnings of a major change in the field that will someday lead to therapeutic interventions for the hearing impaired. Although promising, it is still unknown whether these regenerated HCs make the correct functional connections with the spiral ganglion. With regard to this point, preservation of SGNs is very important and has implications for cochlear implants.

Based on results now being generated by molecular biologists, virologists and stem cell biologists, pure biological approaches to treatment of hearing loss may become ascendant as the choice of treatment in the future.

Acknowledgements

We thank Professor Kaoru Ogawa for his helps. This manuscript was supported by funds of the Researches on Sensory and Communicative Disorders from Japanese Health and Welfare and Labor Administration Grant (H16 sensory organ 008).

References

1. Forge, A., Li, L., Corwin, J. T. & Nevill, G. *Science* **259**, 1616-9 (1993).
2. Forge, A. & Schacht, J. *Audiol Neurootol* **5**, 3-22 (2000).
3. Matsui, J. I., Gale, J. E. & Warchol, M. E. *J Neurobiol* **61**, 250-66 (2004).
4. Ogita, K., Matsunobu, T. & Schacht, J. *Neuroreport* **11**, 859-62 (2000).
5. Matsunobu, T., Ogita, K. & Schacht, J. *Neuroscience* **123**, 1037-43 (2004).
6. Shizuki, K., Ogawa, K., Matsunobu, T., Kanzaki, J. & Ogita, K. *Neurosci Lett* **320**, 73-6 (2002).
7. Camandola, S., Poli, G. & Mattson, M. P. *J Neurochem* **74**, 159-68 (2000).
8. Mattson, M. P., Culmsee, C. & Yu, Z. F. *Cell Tissue Res* **301**, 173-87 (2000).
9. Shoji, F., Yamasoba, T., Magal, E., Dolan, D. F., Altschuler, R. A. & Miller, J. M. *Hear Res* **142**, 41-55 (2000).
10. Yagi, M., Magal, E., Sheng, Z., Ang, K. A. & Raphael, Y. *Hum Gene Ther* **10**, 813-23 (1999).
11. Hakuba, N., Watabe, K., Hyodo, J., Ohashi, T., Eto, Y., Taniguchi, M., Yang, L., Tanaka, J., Hata, R. & Gyo, K. *Gene Ther* **10**, 426-33 (2003).
12. Duan, M., Agerman, K., Ernfors, P. & Canlon, B. *Proc Natl Acad Sci U S A* **97**, 7597-602 (2000).
13. Yamasoba, T., Schacht, J., Shoji, F. & Miller, J. M. *Brain Res* **815**, 317-25 (1999).
14. Ohinata, Y., Miller, J. M. & Schacht, J. *Brain Res* **966**, 265-73 (2003).
15. Yamashita, D., Jiang, H. Y., Schacht, J. & Miller, J. M. *Brain Res* **1019**, 201-9 (2004).
16. Schacht, J. *Otolaryngol Head Neck Surg* **118**, 674-7 (1998).
17. Yamane, H., Nakai, Y., Takayama, M., Iguchi, H., Nakagawa, T. & Kojima, A. *Eur Arch Otorhinolaryngol* **252**, 504-8 (1995).
18. Cotanche, D. A. *Audiol Neurootol* **4**, 271-85 (1999).
19. Warchol, M. E., Lambert, P. R., Goldstein, B. J., Forge, A. & Corwin, J. T. *Science* **259**, 1619-22 (1993).
20. Rubel, E. W., Dew, L. A. & Roberson, D. W. *Science* **267**, 701-7 (1995).
21. Staecker, H. & Van De Water, T. R. *Curr Opin Neurobiol* **8**, 480-7 (1998).
22. Fekete, D. M., Muthukumar, S. & Karagogeos, D. *J Neurosci* **18**, 7811-21 (1998).
23. Adler, H. J. & Raphael, Y. *Neurosci Lett* **205**, 17-20 (1996).
24. Roberson, D. W., Alosi, J. A. & Cotanche, D. A. *J Neurosci Res* **78**, 461-71 (2004).
25. Zheng, J. L., Keller, G. & Gao, W. Q. *J Neurosci* **19**, 2161-70 (1999).

26. Ryan, A. F. *Curr Top Dev Biol* **57**, 449-66 (2003).
27. Lanford, P. J., Lan, Y., Jiang, R., Lindsell, C., Weinmaster, G., Gridley, T. & Kelley, M. W. *Nat Genet* **21**, 289-92 (1999).
28. Woods, C., Montcouquiol, M. & Kelley, M. W. *Nat Neurosci* (2004).
29. Kanzaki, S., Kawamoto, K., Oh, S. H., Stover, T., Suzuki, M., Ishimoto, S., Yagi, M., Miller, J. M., Lomax, M. I. & Raphael, Y. *Audiol Neurootol* **7**, 161-4 (2002).
30. Zheng, J. L., Helbig, C. & Gao, W. Q. *J Neurosci* **17**, 216-26 (1997).
31. Yamashita, H. & Oesterle, E. C. *Proc Natl Acad Sci U S A* **92**, 3152-5 (1995).
32. Kuntz, A. L. & Oesterle, E. C. *J Comp Neurol* **399**, 413-23 (1998).
33. Chen, P. & Segil, N. *Development* **126**, 1581-90 (1999).
34. Cheng, M., Olivier, P., Diehl, J. A., Fero, M., Roussel, M. F., Roberts, J. M. & Sherr, C. J. *Embo J* **18**, 1571-83 (1999).
35. Lowenheim, H., Furness, D. N., Kil, J., Zinn, C., Gultig, K., Fero, M. L., Frost, D., Gummer, A. W., Roberts, J. M., Rubel, E. W., Hackney, C. M. & Zenner, H. P. *Proc Natl Acad Sci U S A* **96**, 4084-8 (1999).
36. Morrison, A., Hodgetts, C., Gossler, A., Hrabe de Angelis, M. & Lewis, J. *Mech Dev* **84**, 169-72 (1999).
37. Zheng, J. L. & Gao, W. Q. *Nat Neurosci* **3**, 580-6 (2000).
38. Shou, J., Zheng, J. L. & Gao, W. Q. *Mol Cell Neurosci* **23**, 169-79 (2003).
39. Zine, A., Aubert, A., Qiu, J., Therianos, S., Guillemot, F., Kageyama, R. & de Ribaupierre, F. *J Neurosci* **21**, 4712-20 (2001).
40. Li, H., Liu, H. & Heller, S. *Nat Med* **9**, 1293-9 (2003).
41. Yamaguchi, M., Saito, H., Suzuki, M. & Mori, K. *Neuroreport* **11**, 1991-6 (2000).
42. Kawaguchi, A., Miyata, T., Sawamoto, K., Takashita, N., Murayama, A., Akamatsu, W., Ogawa, M., Okabe, M., Tano, Y., Goldman, S. A. & Okano, H. *Mol Cell Neurosci* **17**, 259-73 (2001).
43. Kojima, K., Takebayashi, S., Nakagawa, T., Iwai, K. & Ito, J. *Acta Otolaryngol Suppl*, 14-7 (2004).
44. Lopez, I. A., Zhao, P. M., Yamaguchi, M., de Vellis, J. & Espinosa-Jeffrey, A. *Int J Dev Neurosci* **22**, 205-13 (2004).
45. Drucker-Colin, R. & Verdugo-Diaz, L. *Cell Mol Neurobiol* **24**, 301-16 (2004).
46. Duggal, N., Schmidt-Kastner, R. & Hakim, A. M. *Brain Res* **768**, 1-9 (1997).
47. Ito, J., Kojima, K. & Kawaguchi, S. *Acta Otolaryngol* **121**, 140-2 (2001).
48. Naito, Y., Nakamura, T., Nakagawa, T., Iguchi, F., Endo, T., Fujino, K., Kim, T. S., Hiratsuka, Y., Tamura, T., Kanemaru, S., Shimizu, Y. & Ito, J. *Neuroreport* **15**, 1-4 (2004).
49. Kojima, K., Murata, M., Nishio, T., Kawaguchi, S. & Ito, J. *Acta Otolaryngol Suppl*, 53-5 (2004).
50. Kohyama, J., Abe, H., Shimazaki, T., Koizumi, A., Nakashima, K., Gojo, S., Taga, T., Okano, H., Hata, J. & Umezawa, A. *Differentiation* **68**, 235-44 (2001).
51. Lindvall, O., Kokaia, Z. & Martinez-Serrano, A. *Nat Med* **10 Suppl**, S42-50 (2004).
52. Kawamoto, K., Ishimoto, S., Minoda, R., Brough, D. E. & Raphael, Y. *J Neurosci* **23**, 4395-400 (2003).
53. Kanzaki, S., Ogawa, K., Camper, S. A. & Raphael, Y. *Hear Res* **169**, 112-20 (2002).
54. Ishimoto, S., Kawamoto, K., Kanzaki, S. & Raphael, Y. *Hear Res* **173**, 187-97 (2002).

55. Kawamoto, K., Oh, S. H., Kanzaki, S., Brown, N. & Raphael, Y. *Mol Ther* **4**, 575-85 (2001).
56. Springer, J. & Kitzman, P. in *Neuroprotective Signal Transduction* (ed. Mattson, M.) 1-21 (Humana Press Inc, Totowa, NJ, 1998).
57. Otte, J., Schunknecht, H. F. & Kerr, A. G. *Laryngoscope* **88**, 1231-46 (1978).
58. Webster, M. & Webster, D. B. *Brain Res* **212**, 17-30 (1981).
59. Altschuler, R. A., Cho, Y., Ylikoski, J., Pirvola, U., Magal, E. & Miller, J. M. *Ann N Y Acad Sci* **884**, 305-11 (1999).
60. Miller, J. M., Chi, D. H., O'Keeffe, L. J., Kruszka, P., Raphael, Y. & Altschuler, R. A. *Int J Dev Neurosci* **15**, 631-43 (1997).
61. Shinohara, T., Bredberg, G., Ulfendahl, M., Pyykko, I., Olivius, N. P., Kaksonen, R., Lindstrom, B., Altschuler, R. & Miller, J. M. *Proc Natl Acad Sci U S A* **99**, 1657-60 (2002).
62. Mitchell, A., Miller, J. M., Finger, P. A., Heller, J. W., Raphael, Y. & Altschuler, R. A. *Hear Res* **105**, 30-43 (1997).
63. Shepherd, R. K. & Hardie, N. A. *Audiol Neurootol* **6**, 305-18 (2001).
64. Araki, S., Kawano, A., Seldon, L., Shepherd, R. K., Funasaka, S. & Clark, G. M. *Laryngoscope* **108**, 687-95 (1998).
65. Li, L., Parkins, C. W. & Webster, D. B. *Hear Res* **133**, 27-39 (1999).
66. Lousteau, R. J. *Laryngoscope* **97**, 836-42 (1987).
67. Hartshorn, D. O., Miller, J. M. & Altschuler, R. A. *Otolaryngol Head Neck Surg* **104**, 311-9 (1991).
68. Leake, P. A., Hradek, G. T., Rebscher, S. J. & Snyder, R. L. *Hear Res* **54**, 251-71 (1991).
69. Hegarty, J. L., Kay, A. R. & Green, S. H. *J Neurosci* **17**, 1959-70 (1997).
70. Miller, A. L., Prieskorn, D. M., Altschuler, R. A. & Miller, J. M. *Brain Res* **966**, 218-30 (2003).
71. Yagi, M., Kanzaki, S., Kawamoto, K., Shin, B., Shah, P. P., Magal, E., Sheng, J. & Raphael, Y. *J Assoc Res Otolaryngol* **1**, 315-25 (2000).
72. Kanzaki, S., Stover, T., Kawamoto, K., Prieskorn, D. M., Altschuler, R. A., Miller, J. M. & Raphael, Y. *J Comp Neurol* **454**, 350-60 (2002).
73. Paasche, G., Gibson, P., Averbeck, T., Becker, H., Lenarz, T. & Stover, T. *Otol Neurotol* **24**, 222-7 (2003).
74. Tateya, I., Nakagawa, T., Iguchi, F., Kim, T. S., Endo, T., Yamada, S., Kageyama, R., Naito, Y. & Ito, J. *Neuroreport* **14**, 1677-81 (2003).
75. Hu, Z., Wei, D., Johansson, C. B., Holmstrom, N., Duan, M., Frisen, J. & Ulfendahl, M. *Exp Cell Res* **302**, 40-7 (2005).

Available online at www.sciencedirect.com
SCIENCE DIRECT®
Hearing Research xxx (2006) xxx–xxx
HEARING RESEARCH
www.elsevier.com/locate/heares

Research paper

p27^{Kip1} deficiency causes organ of Corti pathology and hearing loss

Sho Kanzaki [b], Lisa A. Beyer [a], Donald L. Swiderski [a], Masahiko Izumikawa [a], Timo Stöver [c], Kohei Kawamoto [d], Yehoash Raphael [a,*]

[a] *Kresge Hearing Research Institute, The University of Michigan Medical School, MSRB III Room-9303, 1150 West Medical Center Drive, Ann Arbor, MI 48109-0648, USA*
[b] *Department of Otolaryngology, Keio University, 35 Shinanomachi, Shinjuku, Tokyo 160-0016, Japan*
[c] *Department of Otolaryngology, Hannover University, Germany*
[d] *Department of Otolaryngology, Kansai Medical University, Osaka, Japan*

Received 30 June 2005; received in revised form 30 December 2005; accepted 18 January 2006

Abstract

p27^{Kip1} (p27) has been shown to inhibit several cyclin-dependent kinase molecules and to play a central role in regulating entry into the cell cycle. Once hair cells in the cochlea are formed, p27 is expressed in non-sensory cells of the organ of Corti and prevents their re-entry into the cell cycle. In one line of p27 deficient mice (p27$^{-/-}$), cell division in the organ of Corti continues past its normal embryonic time, leading to continual production of cells in the organ of Corti. Here we report on the structure and function of the inner ear in another line of p27 deficient mice originating from the Memorial Sloan-Kettering Cancer Center. The deficiency in p27 expression of these mice is incomplete, as they retain expression of amino acids 52–197. We determined that mice homozygote for this mutation had severe hearing loss and their organ of Corti exhibited an increase in the number of inner and outer hair cells. There also was a marked increase in the number of supporting cells, with severe pathologies in pillar cells. These data show similarities between this p27^{Kip1} mutation and another, previously reported null allele of this gene, and suggest that reducing the inhibition on the cell cycle in the organ of Corti leads to pathology and dysfunction. Manipulations to regulate the time and place of p27 inhibition will be necessary for inducing functionally useful hair cell regeneration.

Keywords: Hair cell; Cell cycle; Deafness; p27^{Kip1}; Mouse

1. Introduction

During embryonic development of the mouse cochlea, the transition from the proliferative stage to the period of hair cell differentiation starts around embryonic day (E) 13 (Chen and Segil, 1999; Lumpkin et al., 2003; Ruben, 1967; Woods et al., 2004). In normal mice, no new cells are added to the sensory epithelium after embryonic day 15. Several cell-cycle regulating proteins have been shown to participate in the transition from proliferation to differentiation. The genes encoding these proteins include p27^{Kip1} (p27), a member of the Cip–Kip family of cyclin-dependent kinases (Chen and Segil, 1999; Lowenheim et al., 1999), Ink4d (Chen et al., 2003) and the retinoblastoma gene Rb1, a tumor suppressor gene (Sage et al., 2005). Other genes that have not yet been identified may also be involved. Better understanding of the gene expression cascade leading to cell-cycle quiescence in the organ of Corti may be instrumental in finding ways to manipulate the cell cycle in this organ and design ways to induce generation of new hair cells to repopulate the deafened organ of Corti.

A previous study found that p27 is an important regulator of progenitor cell proliferation during development of the brain, retina and other tissues (Assoian, 2004). p27 was found to be upregulated during the late G2 or early G1 phase of the cell cycle (Koff and Polyak, 1995). Over-expression of

* Corresponding author. Tel.: +1 734 936 9386; fax: +1 734 615 8111/647 2563.
E-mail address: yoash@umich.edu (Y. Raphael).

0378-5955/$ - see front matter © 2006 Published by Elsevier B.V.
doi:10.1016/j.heares.2006.01.014

p27 in progenitor cells leads to their premature exit from the cell cycle (Tarui et al., 2005). A complete deletion of the gene leads to gigantism and excess proliferation in several tissues including hematopoietic, pituitary and ovarian cells (Fero et al., 1996). In the cochlea of mice lacking one or both alleles of p27, the proportion of mitotic cells in the cochlea is increased (Chen and Segil, 1999; Lowenheim et al., 1999). These mice exhibit excessive number of cells in the organ of Corti (Chen and Segil, 1999; Lowenheim et al., 1999) and impaired hearing (Lowenheim et al., 1999).

The deletion studies mentioned above examined the effects of a complete deletion of the gene (Fero et al., 1996; Nakayama et al., 1996). In this study, we examine the effects of a less severe mutation generated at the Memorial Sloan-Kettering Cancer Center (Kiyokawa et al., 1996). This mutation is a partial deletion eliminating the first 51 amino acids, resulting in a hypomorphic allele with reduced ability to inhibit cyclin-dependent kinase activity (Kiyokawa et al., 1996). Our goal was to characterize the inner ear phenotype of transgenic mice with this incomplete p27 deficiency. Using acoustic brainstem response (ABR) audiometry, we determined that their hearing is severely impaired. Using SEM, TEM and cytochemistry, we determined that the sensory epithelium has pathological changes in both hair cells and supporting cells.

2. Materials and methods

2.1. Animals and genotype analysis

p27 deficient mice (Kiyokawa et al., 1996) were kindly provided by Dr. Koff (The Memorial Sloan-Kettering Cancer Center, NY). The genetic background of these mice was hybrid 129SvJ with C57Bl/6. The three different genotypes used were $p27^{+/+}$ (wild-type, normal control $N = 4$), $P27^{+/-}$ (heterozygous $N = 5$) and $P27^{-/-}$ (homozygous for the p27 deficiency $N = 5$). Animal care and handling were approved by the University of Michigan Institutional Committee on the Use and Care of Animals and were performed using accepted veterinary standards. Mice were sacrificed at the age of 21 days (P21) and genotyped by PCR using tail DNA as previously reported (Kiyokawa et al., 1996), with the following DNA fragments: 294, 61 (bp) for $P27^{-/-}$, 294, 223, 71, 61 (bp) for $P27^{+/-}$, 223, 71 (bp) for wild-types.

2.2. ABR analysis

To assess ABR thresholds, mice ($P27^{-/-}$ $N = 3$; $P27^{+/-}$ $N = 3$, and $p27^{+/+}$ $N = 2$) were tested at 4, 10 and 20 kHz. Animals were anesthetized with mixture of xylazine (1.25 mg/g) and ketamine (62.5 mg/g). An active needle electrode was subdermally inserted at the vertex, along the dorsal midline of the scalp between the external auditory canals. The reference electrode was placed below the pinna of the left ear and the ground electrode was inserted below the contralateral ear.

The sound stimulus consisted of a 15 ms tone burst with rise–fall time of 1 ms. The sound stimuli were delivered from an encased, shielded Beyer earphone through a 13 mm tube into the ear canal. Response waveforms (100,000 gain, filtered from 0.3 to 3 kHz) were averaged (1024 epochs) using a Tucker Davis data acquisition system. The response threshold was defined as the interpolated value between the last level in which a response was presented and 5 dB lower where no response was observed.

We performed ANOVA to test for differences in ABR thresholds among the three genotypes at each frequency. Because three frequencies were tested, we used a Bonferroni-adjusted critical p-value of 0.015. When the ANOVA found a significant difference, unpaired t-tests were used to determine which genotypes were significantly different, again using a Bonferroni-adjusted critical p-value of 0.015.

2.3. Scanning electron microscopy (SEM)

We used two 21-day old animals from each genotype ($P27^{-/-}$, $P27^{+/-}$ and $p27^{+/+}$). Animals were anesthetized and perfused with 2% paraformaldehyde and 2% glutaraldehyde in 0.15 M cacodylate. Cochleae were removed and fixed in the same fixative overnight. Tissues were then incubated in 1% osmium tetroxide for 60 min. Samples were dehydrated in ethanol and critical point dried with CO_2 in a SamDri 790 (Tousimis, Rockville, MD). Samples were mounted on stubs, sputter coated with gold using Polaron 5100 (Polaron Equipment Limited, Watford Hertfordshire, UK) and examined on a Phillips FEI XL30FEG SEM. The entire cochlear length was analyzed and the images presented are from the lower apical turn.

2.4. Transmission electron microscopy (TEM)

Cochleae from two mice of each phenotype ($P27^{-/-}$, $P27^{+/-}$ and $p27^{+/+}$) were used. Animals were anesthetized and perfused with 2% paraformaldehyde and 2% glutaraldehyde in 0.15M cacodylate. Cochleae were removed, osmicated (as above) and decalcified until soft (approximately one week). Tissues were stained with aqueous uranyl acetate, dehydrated in ethanol followed by propylene oxide, and embedded in Embed 812 epoxy resin (Electron Microscopy Sciences, Washington, PA). Epon blocks were sectioned using a Leica Ultracut R ultramicrotome using a diamond knife (slice thickness; 80 nm). Sections from the lower apical turn were collected on grids (Electron Microscope Sciences, 200 Hex mesh T/B). The grids were stained with uranyl acetate and lead citrate and examined on a Phillips CM 100 TEM.

2.5. Whole-mount analysis

We used a phalloidin stain to label F-actin in the tissue in order to enhance identification of cell types and their organization in the sensory epithelium (Raphael et al.,

1994b) and Hoechst to stain DNA and visualize nuclei (Raphael, 1993). Animals (three from each genotype) were deeply anesthetized, decapitated, and their temporal bones were removed. The cochleae were excised, the bony capsule removed and tissues were fixed in 4% paraformaldehyde for 2 h. Further dissection was performed to remove the lateral wall tissues and the tectorial membrane. The samples were permeabilized with 0.3% Triton X-100 in PBS for 5 min, and incubated for 30 min in rhodamine conjugated phalloidin (Jackson Immunoresearch, West grove, PA) diluted 1:100 in PBS. Stained whole-mount of the apical turn were mounted on microscope slides with Crystal/Mount (Biomedia, Foster City, CA), and examined with a laser scanning confocal microscope (BioRad MRC600) with a 63 × N/A 1.4 objective attached to Nikon Diaphot microscope. Z-series images (1 μm interval) were taken at the lower apical turn, starting from the apical luminal aspect of the sensory epithelium, spanning the entire epithelial layer and terminating at the extracellular matrix beneath the epithelium. Files were converted and stored as TIFF files. The Z-series stack was then converted to individual image files using NIH Image.

Two ears of each genotype were also stained with Hoechst 33342 (Molecular Probes, Eugene, OR) and photographed with epi-fluorescence (Leica DMRB upright photomicroscope) at several focal planes. Images at the UV wavelength were obtained from the lower apical turn with a digital monochrome Spot camera (Diagnostic Instruments, Inc., Sterling Heights, MI). The number of nuclei in the outer hair cell area was counted in all focal planes of the epithelium.

2.6. Image processing

We used Adobe Photoshop for adjustment of image contrast, insert symbols and letters for labels and crop images for preparation of figure panels.

3. Results

Confocal microscopy images of phalloidin stained whole-mounts of the organ of Corti reveals that the homozygous mutant mouse ($p27^{-/-}$) has hair cells and supporting cells, but that their organization and appearance are abnormal (Fig. 1A). In several locations along the cochlear duct, two rows of inner hair cells and four rows of outer hair cells were observed, rather than the normal one and three rows, respectively. The morphology of the supporting cells in $p27^{-/-}$ is also abnormal. This is most evident in the pillar cells, where the thick actin filaments near the apical surfaces of the cells are disorganized. In heterozygotes ($p27^{+/-}$, Fig. 1B), the organization of the mosaic of the auditory epithelium is much closer to that seen in the wild-type ($p27^{+/+}$, Fig. 1C). The $p27^{+/-}$ mice display a nearly normal organization of hair cells, but the junctional actin in supporting cells is slightly altered, especially in pillar cells. In wild-type animals (Fig. 1C) the organization of the pillar cells and the rows of hair cells is regular and the number of cells in each row is usually constant, with one row of inner hair cells and three rows of outer hair cells.

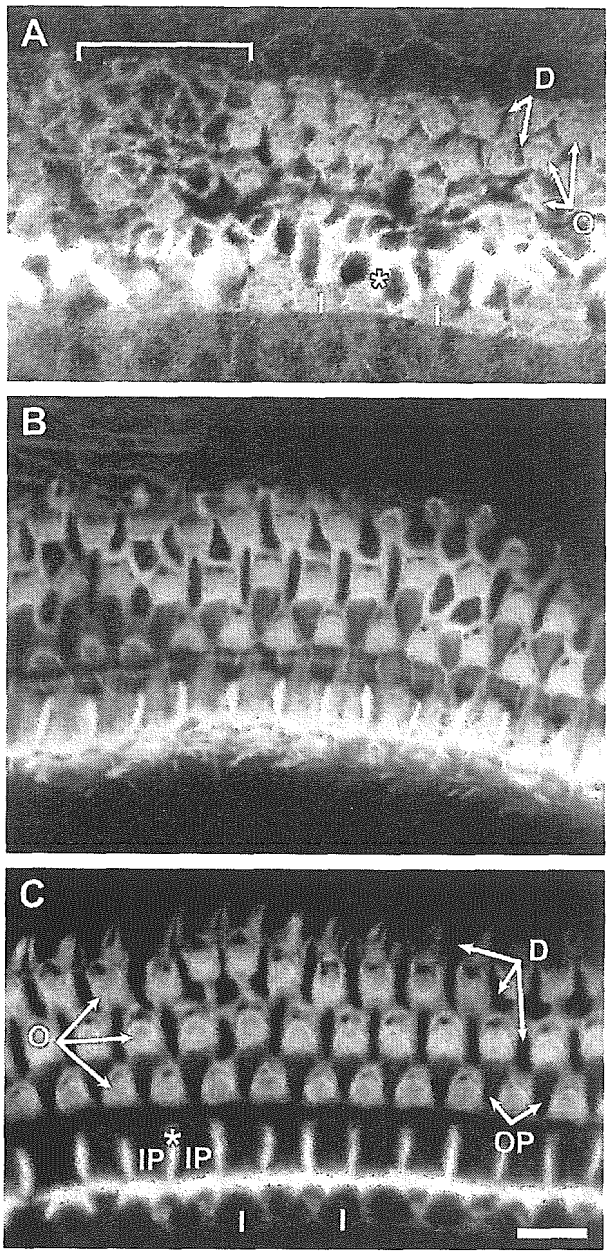

Fig. 1. Confocal microscopic images of phalloidin stained whole-mounts of the organ of Corti from $p27^{-/-}$ homozygouse mutant (A), $p27^{+/-}$ heterozygous (B) and $p27^{+/+}$ wild-type (C) mice. A: Several outer hair cells are missing (bracket). Remaining outer hair cells (O arrows point to outer hair cell rows 1–3) are in disarray. The actin bundles which represent intercellular junctions between inner pillar cells reveal disorganization of the apical portions of pillar cells (asterisk). The typical dumbbell shape of the Deiters cell apical surface is abnormal (D arrows). I denotes inner hair cells. B: Outer hair cell and pillar cells are closer to normal but their organization is imperfect. C: Actin bundles depict the typical normal organization of hair cells and supporting cells of the organ of Corti. D arrows point to three rows of Deiters cells, O arrows point to three rows of outer hair cells, OP point to outer pillar cells, IP denotes inner pillar, asterisk points to the junctional actin between inner pillar cells, I marks inner hair cell. Scale bar: 10 μm.

The nuclei of the auditory epithelium were analyzed in whole-mounts of the organ of Corti of wild-type and $p27^{-/-}$ animals. Nuclei in the outer hair cell area of the normal organ of Corti are round and arranged in clear and distinctive three rows, visible beneath the luminal surface (Fig. 2). Immediately beneath the three rows of outer hair cell nuclei, are the Deiters cell nuclei. Moving further towards the basilar membrane reveals a dense aggregation of spindle-shaped nuclei representing mesothelial cells residing underneath the epithelium, lining the scala tympani (Fig. 2D). Thus, two distinct rows of nuclei are observed above the mesothelial layer in the outer hair cell area of the normal cochlea. In the $p27^{-/-}$ mutant ears (Fig. 3), hair cell nuclei were seen in three rows of that were somewhat less well organized than in the normal ear (Fig. 3B, compare to Fig. 2B). The contour of the nuclei was nearly round but many nuclei showed slightly distorted shape (Fig. 3B). When observing lower focal planes (towards the basilar membrane), the $p27^{-/-}$ ear contained numerous nuclei at all focal planes under the luminal surface (Fig. 3C–E). Thus, nuclei in the Deiters cell area appeared to be present at more than one focal plane.

Nuclei were counted in an area measuring 50×50 μm in the outer hair cell region. Counts in three such areas averaged a total of 43 nuclei in the wild-type animals versus 68 nuclei in $p27^{-/-}$ animals, representing an increase of more than 50%. Because some hair cell loss is already apparent at this age, we infer that the increase in the number of nuclei represents mostly an increase in the number of supporting cells (Fig. 1A).

SEM confirms the presence of supernumerary hair cells and disorganized apical surface of supporting cells (Fig. 4). In the $p27^{-/-}$ ears, the normal organization of pillar and Deiters cells could not be observed (Fig. 4A). The $p27^{+/-}$ ears (Fig. 4B) exhibited an intermediate phenotype between the wild-type and the $p27^{-/-}$ ears. Individual hair cells did not appear perfectly normal in the mutant animals (Fig. 5) but the differences between normal wild-type ears and mutants was not as marked as that seen in supporting cells.

In cross sections, no tunnel of Corti or Nuel space are observed (Fig. 6). Instead, numerous cells occupy these

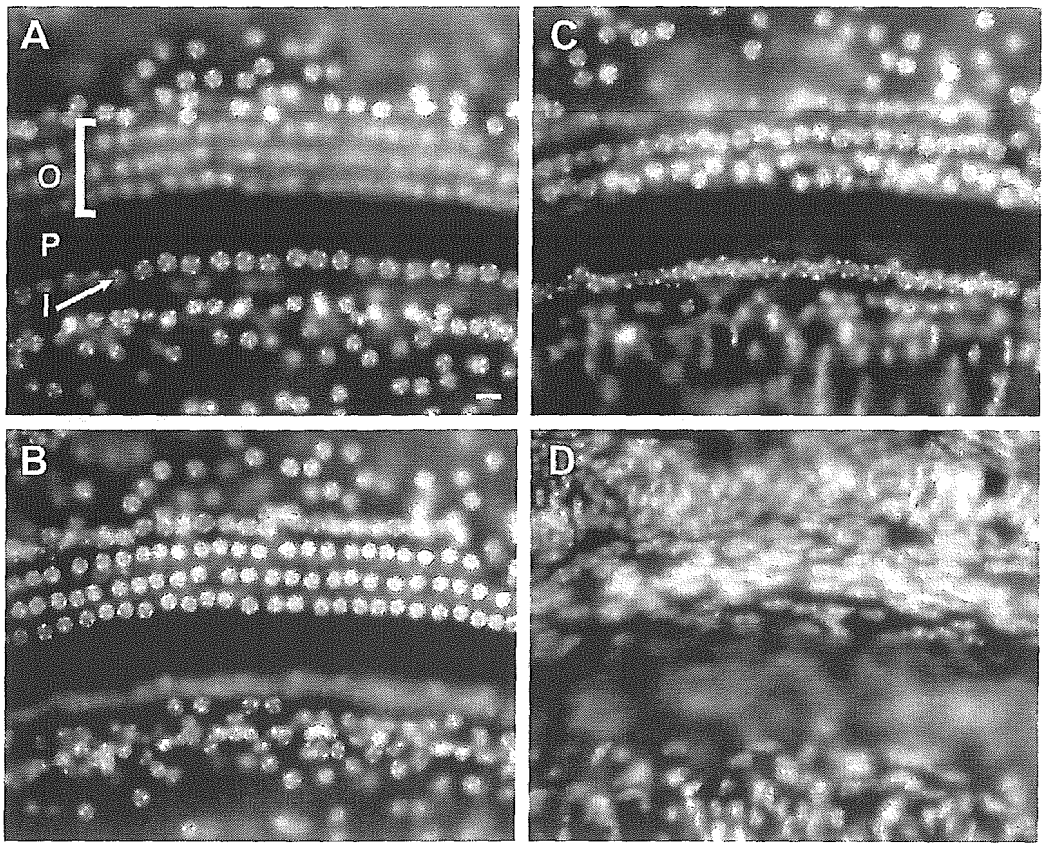

Fig. 2. The normal organ of Corti contains two distinctive planes of nuclei in the outer hair cell area. Whole-mounts of the organ of Corti of a wild-type $p27^{+/+}$ mouse stained with Hoechst and photographed at four focal planes starting above the nuclei of outer hair cells (A) and descending towards the area under the basilar membrane (D). A: nuclei of inner hair cells (I) and Hensen cells (at upper end of bracket) flank the outer hair cell area above the focal plane of outer hair cell nuclei (P shows area of pillar cell heads). B: Outer hair cell nuclei are arranged in three distinctive and well organized rows. The perimeter of outer hair cell nuclei is round and smooth. C: At a lower focal plane, nuclei of Deiters cells (supporting cell) are clearly identified. Nuclei of these cells are slightly larger than outer hair cell nuclei. D: The next set of nuclei visible under the Deiters cell nuclei are spindle-shaped nuclei of mesothelial cells residing under the basilar membrane. Scale bar (in A, for A–D): 10 μm.

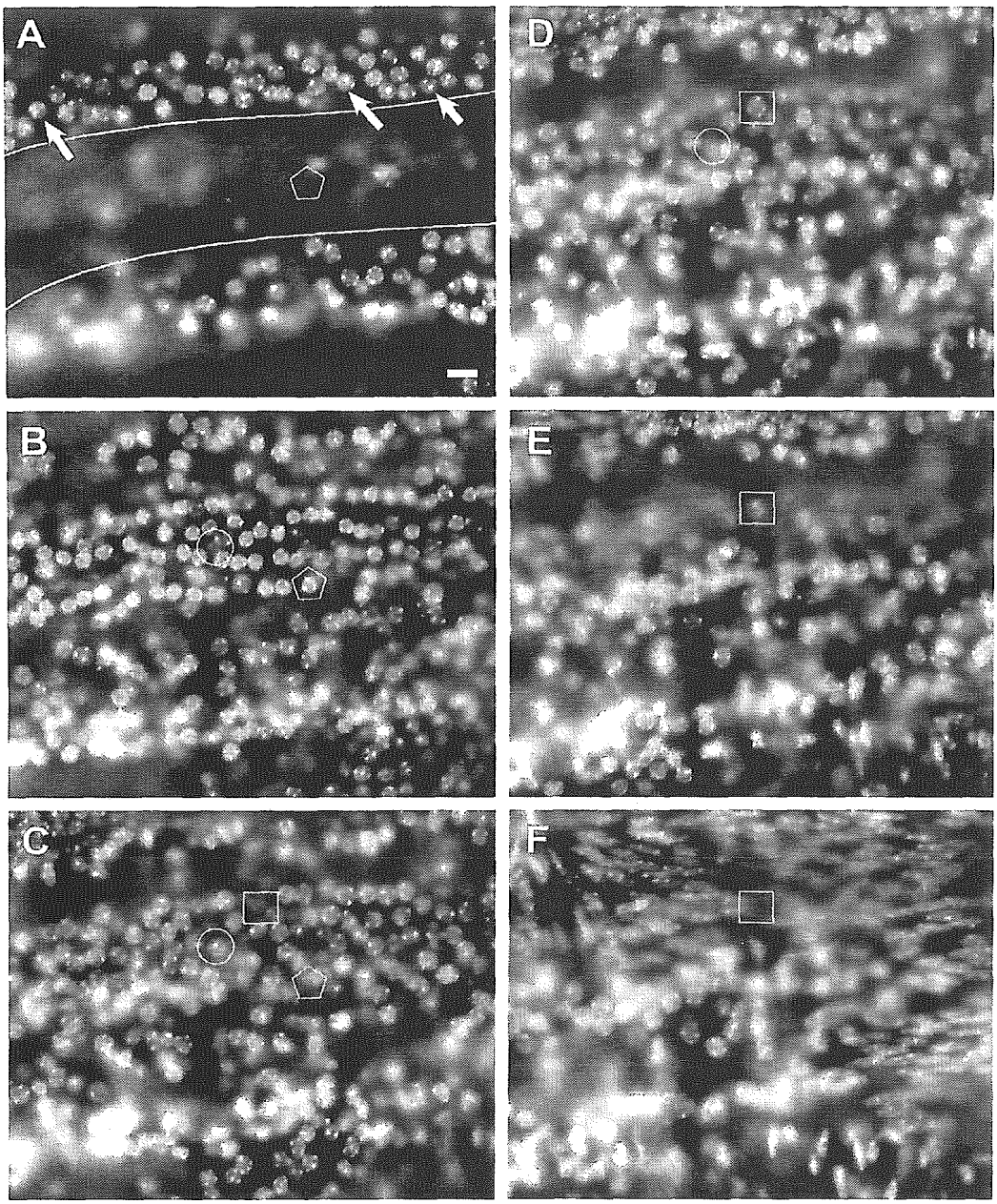

Fig. 3. In the outer hair cell area of $p27^{-/-}$ mice the nuclei are spread throughout the epithelium at all focal planes, as depicted by Hoechst stained whole-mount photographed at six different planes (A–F) from just under the luminal surface (A) to under the basilar membrane (F). A: Immediately beneath the luminal surface there are no visible nuclei in the outer hair cell area (between the border lines) but Hensen cell nuclei are seen in the lateral aspect of the organ of Corti (arrows) and inner hair cell nuclei are in the medial side. The pentagon is a selected area with no nucleus, corresponding the nucleus present in B. B: Outer hair cell nuclei appear at a lower focal plane. The perimeter of the nuclei is slightly rough and the spherical shape is less well defined than in normal mice (compare to Fig. 2B). The circle depicts an area with no nucleus, corresponding to the area in C where a nucleus appears. C: Numerous supporting cell nuclei are visible under the level of the outer hair cell nuclei. Supporting cell nuclei are slightly larger than outer hair cell nuclei. The square introduces an area devoid of a nucleus, in which a lower focal plane will contain a nucleus (in D). D: Many additional supporting cell nuclei are seen in a lower focal plane. E: A lower focal plane in which most nuclei shown in D disappear, and others appear. This is the lowest focal plane in the epithelium, immediately above the basilar membrane. F: Spindle shape nuclei (mesothelial cell nuclei) appear at a lower focal plane just beneath the basilar membrane. Scale bar (in A, for A–F): 10 μm.

fluid spaces (Fig. 6A). These cells could be pillar cells and Deiters cells and/or progenitor cells that are in the process of differentiating or dividing. The morphology of outer hair cells is pathological (Fig. 6A) but inner hair cells appear relatively normal (Fig. 6A and B). Supporting cell nuclei are not restricted to a single focal plane below the row of outer hair cell nuclei, but instead, they are observed in multiple levels in the epithelium (Fig. 6A, compare to Fig. 3C–E). Some of the supporting cell nuclei reside in the basal region of the epithelium, adjacent to the basilar

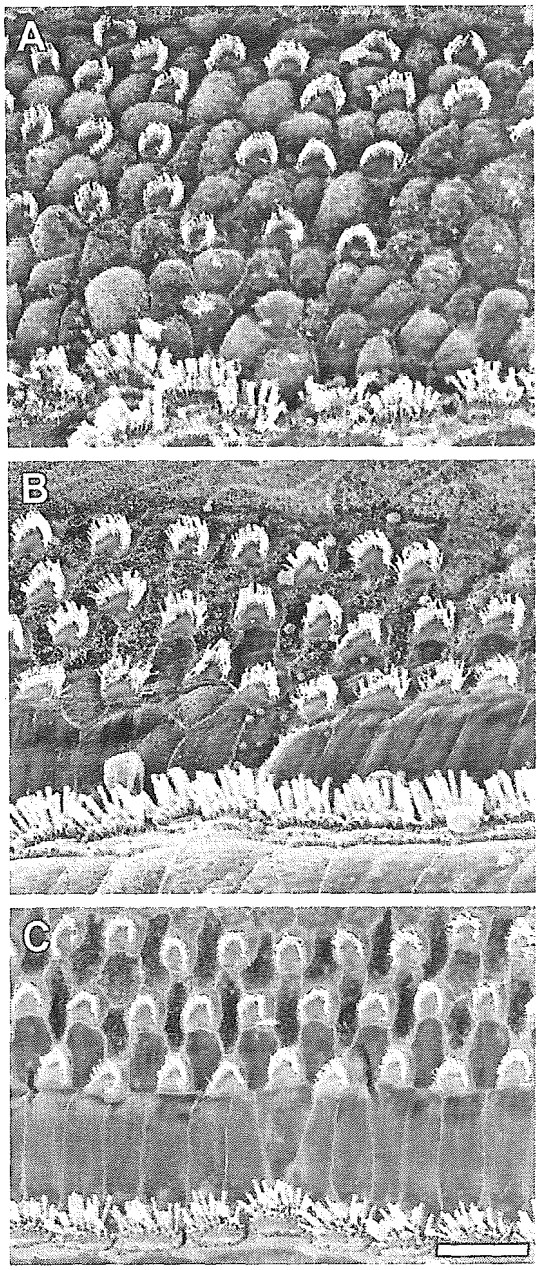

Fig. 4. SEM micrographs of the surface of the auditory epithelium in $p27^{-/-}$ (A), $p27^{+/-}$ (B) and $p27^{+/+}$ (C) mice. A: Inner hair cells are not well organized and a few of them form a second row. Outer hair cells are poorly organized and four rows can be discerned. The surface of supporting cells between outer hair cells is wider than usual and the cell borders are abnormal. The surface of the pillar cells has many more cells than in normal ears and lacks clear organization. B: The appearance of hair cells and supporting cells is close to normal. The number of cell rows is normal in both inner and outer hair cells. Pillar cell organization is slightly imperfect. C: The morphology of hair cells and supporting cells is normal. Magnification bar: 10 μm.

membrane. These nuclei appear to be attached to the basal lamina and flatten against it (Fig. 6A).

ABR audiometry (Fig. 7) shows that homozygous $p27^{-/-}$ mice have severe hearing loss at the three tested frequencies (4, 10 and 20 kHz) whereas heterozygous mice are much closer to wild-type, which exhibit normal hearing. ANOVA indicates that there are statistical differences in ABR thresholds among genotypes at each frequency. *T*-tests indicate that homozygous mutants have significantly higher thresholds than heterozygotes at each frequency. Although heterozygotes tend to have higher thresholds than wild-types, the differences were not significant at any of the tested frequencies.

4. Discussion

Overall, the structure and function of the inner ears of mice described in this report are similar to previous reports of different p27 mutations. We found that auditory function is severely impaired in $p27^{-/-}$ mice, and appears to be slightly impaired in the heterozygotes. The morphology of the sensory epithelium is consistent with the functional data and follows a similar hierarchy of pathology. Hair cells were present in all three genotypes and the most prominent pathology appeared to be in the number and organization of supporting cells.

The functional deficit in the $p27^{-/-}$ mice may be related to more than one pathology. The irregular organization of the outer hair cell area is incompatible with a normal "active" cochlea. As such, a threshold shift of 50–60 dB is expected due to the outer hair cell pathology (Dallos and Harris, 1978). In addition, it is likely that differentiation of the inner hair cells is incomplete due to crowding. Because the mosaic organization of the organ of Corti is dependent on both cell types, it is difficult to determine which cell is responsible for the primary pathology. Furthermore, p27 has a role in normal differentiation of neuronal tissues (Baldassarre et al., 2000; Sasaki et al., 2000), so the innervation of the auditory hair cells in p27 deficient mice also is likely to be abnormal.

The data obtained from cross sections of the $p27^{-/-}$ organ of Corti suggest that the excess in cell number is more prominent in supporting cells. The observation that some supporting cell nuclei are positioned flat against the basilar membrane indicates that these cells may be in s-phase, as previously shown in the regenerating auditory epithelium of birds (Raphael et al., 1994a). This suggests that new cells are still being added to the epithelium in these 21-day-old mice, more than four weeks after mitosis in the sensory epithelium is normally completed. It is possible that some of these newly-added cells differentiate into new hair cells.

Mice homozygous for the other p27 mutation (Nakayama et al., 1996) are also severely hearing impaired (Lowenheim et al., 1999), yet the pathology is not identical to that in the mouse we now describe. The organ of Corti of both p27 mutants is disorganized and includes supernumerary supporting cells and hair cells. The pathology and hearing impairment are severe in homozygotes of both mutants, but the heterozygotes seem to be slightly different. Elevated thresholds are seen in the heterozygotes of the partially deleted gene (hypomorphic mutation reported

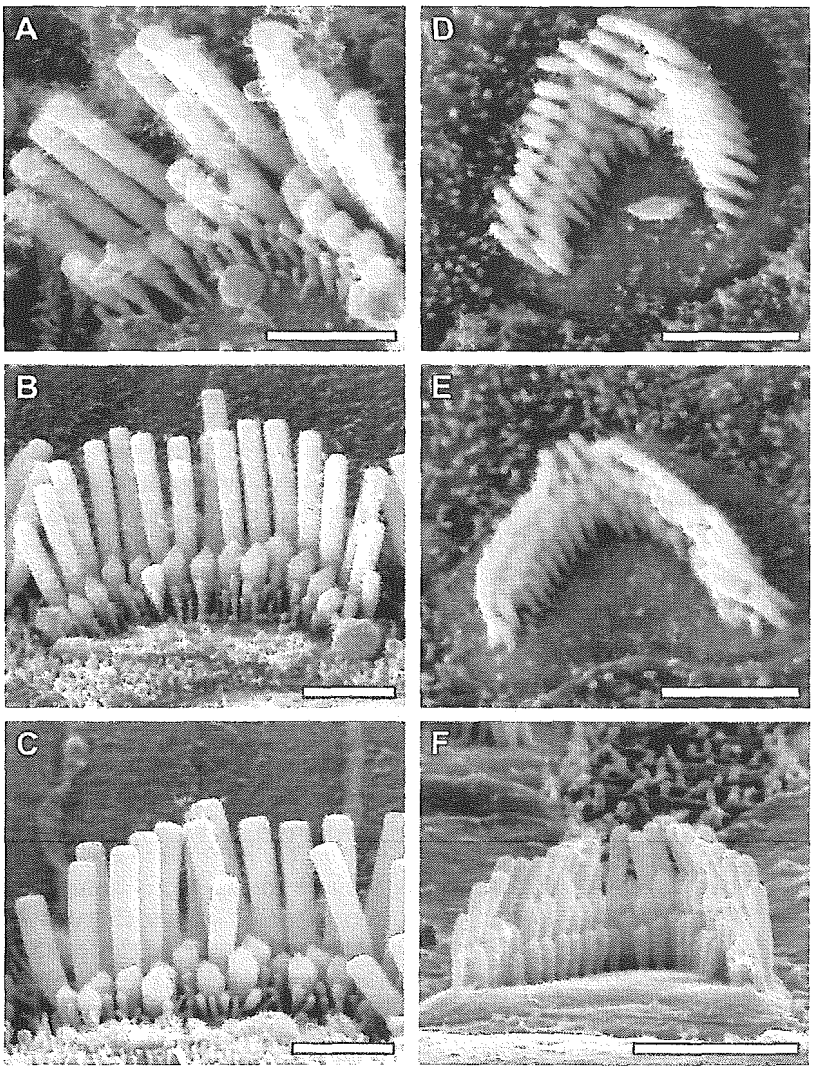

Fig. 5. SEM of apical surface of inner hair cells (A–C) and outer hair cells (D–F) of $p27^{-/-}$ (A and D), $p27^{+/-}$ (B and E) and $p27^{+/+}$ mice (C and F). The number, height and organization of stereocilia are similar in all three genotypes, but $p27^{-/-}$ hair cells appear to have slightly disorganized stereocilia, especially on the inner hair cell. Scale bars: 2 μm.

here) but not in the heterozygotes of the completely deleted p27 gene (Lowenheim et al., 1999). We speculate that the slight hearing loss in the heterozygotes of the hypomorphic deletion (studied here) is due to a dominant negative role assumed by the truncated protein in the organ of Corti. Reduced compensatory role of other genes may also play a role in the pathology seen in the hypomorphic deletion. Another possibility is that the genetic background of these hybrid mice plays a role in the severity of the heterozygote phenotype.

The genetic background of the $p27^{Kip1}$ mutant animals used in this study was hybrid 129SvJ with C57Bl/6. Both strains carry a synonymous single-nucleotide polymorphism (SNP) in exon 7 of *Cdh23* that is significantly associated with *Ahl* (Noben-Trauth et al., 2003). However, mice used in this study were 21 days old, much younger than the expected onset of age-related hearing loss, thus the pathology they exhibit is likely independent of *Ahl*.

Although the unregulated production of cells in the organ of Corti appears to involve a functional deficit, the results do have implications for designing controlled methods for inducing hair cell regeneration in the mammalian cochlea. A better understanding of cell cycle regulation in the organ of Corti may lead to enhanced ability to manipulate the genes involved in this process. Regulated inhibition of p27, Rb1 (Sage et al., 2005) or other cell cycle proteins may produce a pulse of cell generation that can be used for reconstructing the pathological organ of Corti. Skp2, a F-box protein that can inhibit p27 by unbiquitination, is present in the inner ear (Dong et al., 2003) and may be used to regulate the levels of p27. To accomplish functionally meaningful hair cell regeneration, it may also be necessary to combine the manipulation of cell cycle with induction of hair cell differentiation by genes such as *Atoh1* (Bermingham et al., 1999; Izumikawa et al., 2005; Shou et al., 2003).

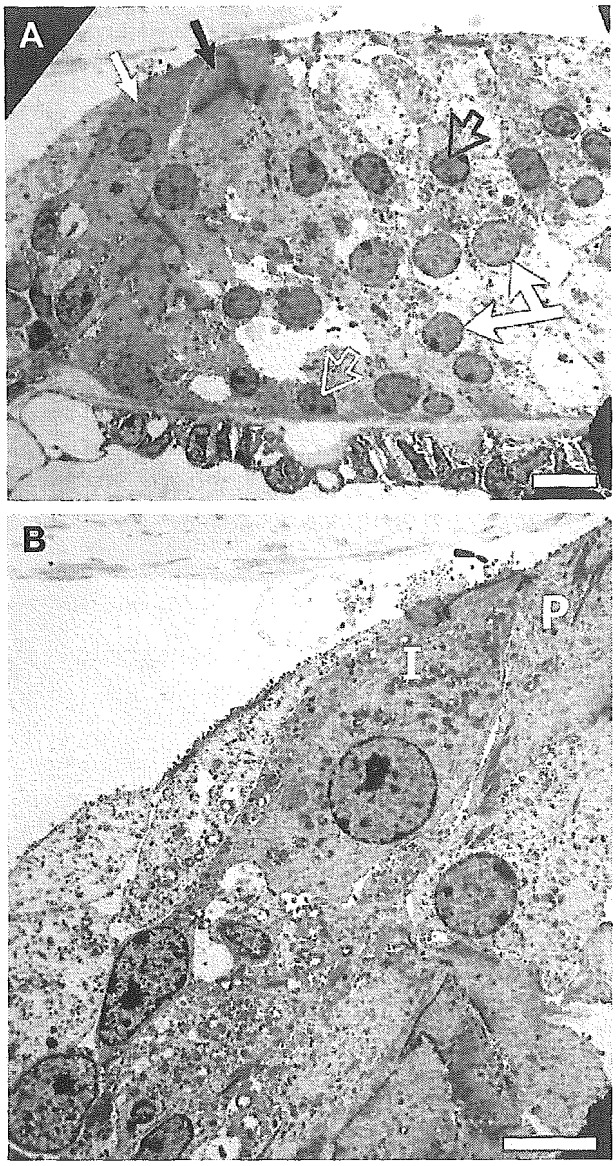

Fig. 6. TEM micrographs of organ of Corti sections in $p27^{-/-}$ cochleae. A: The inner hair cell (white filled arrow) has relatively normal morphology. Outer hair cells nuclei are present (black open arrow) but the cells bodies are pathological. Pillar cell (black filled arrow) morphology in the apical domain is abnormal, and the basal domain is not clearly identified. Supporting cell nuclei appear under the outer hair cells (double arrow) and in additional locations, including close proximity to the basilar membrane. One nucleus is flattened against the basal lamina (white open arrow). B: An inner hair cell (I) with relatively normal morphology. The adjacent pillar cell (P) appears undifferentiated and lacks typical pillar shape and cytoskeletal components. Scale bars: 10 μm in A and 5 μm in B.

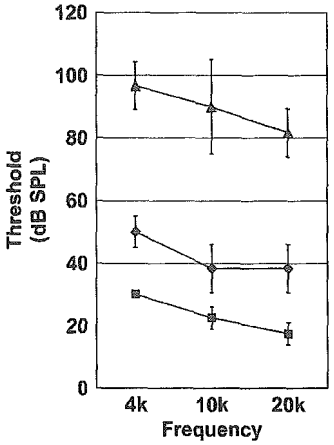

Fig. 7. ABR thresholds for the three genotypes in each of the three tested frequencies. Data points represent the mean thresholds and standard deviation. Squares are for $p27^{+/+}$, diamonds represent $p27^{+/-}$ and triangles for $p27^{-/-}$.

Acknowledgements

We thank Graham Atkin for technical assistance. This work was supported by Berte and Alan Hirschfield, the CHD, GM and the UAW, a grant from the Japan Ministry of Health and Labor H16-008, and NIH NIDCD Grants R01-DC05053 and R01-DC01634 and P30 DC05188.

References

Assoian, R.K., 2004. Stopping and going with p27kip1. Dev Cell 6, 458–459.

Baldassarre, G., Boccia, A., Bruni, P., Sandomenico, C., Barone, M.V., Pepe, S., Angrisano, T., Belletti, B., Motti, M.L., Fusco, A., Viglietto, G., 2000. Retinoic acid induces neuronal differentiation of embryonal carcinoma cells by reducing proteasome-dependent proteolysis of the cyclin-dependent inhibitor p27. Cell Growth Differ. 11, 517–526.

Bermingham, N.A., Hassan, B.A., Price, S.D., Vollrath, M.A., Ben-Arie, N., Eatock, R.A., Bellen, H.J., Lysakowski, A., Zoghbi, H.Y., 1999. Math1: an essential gene for the generation of inner ear hair cells. Science 284, 1837–1841.

Chen, P., Segil, N., 1999. p27(Kip1) links cell proliferation to morphogenesis in the developing organ of Corti. Development 126, 1581–1590.

Chen, P., Zindy, F., Abdala, C., Liu, F., Li, X., Roussel, M.F., Segil, N., 2003. Progressive hearing loss in mice lacking the cyclin-dependent kinase inhibitor Ink4d. Nat. Cell Biol. 5, 422–426.

Dallos, P., Harris, D., 1978. Properties of auditory nerve responses in absence of outer hair cells. J. Neurophysiol. 41, 365–383.

Dong, Y., Nakagawa, T., Endo, T., Kim, T.S., Iguchi, F., Yamamoto, N., Naito, Y., Ito, J., 2003. Role of the F-box protein Skp2 in cell proliferation in the developing auditory system in mice. Neuroreport 14, 759–761.

Fero, M.L., Rivkin, M., Tasch, M., Porter, P., Carow, C.E., Firpo, E., Polyak, K., Tsai, L.H., Broudy, V., Perlmutter, R.M., Kaushansky, K., Roberts, J.M., 1996. A syndrome of multiorgan hyperplasia with features of gigantism, tumorigenesis, and female sterility in p27(Kip1)-deficient mice. Cell 85, 733–744.

Izumikawa, M., Minoda, R., Kawamoto, K., Abrashkin, K.A., Swiderski, D.L., Dolan, D.F., Brough, D.E., Raphael, Y., 2005. Auditory hair cell replacement and hearing improvement by Atoh1 gene therapy in deaf mammals. Nat. Med. 11, 271–276.

Kiyokawa, H., Kineman, R.D., Manova-Todorova, K.O., Soares, V.C., Hoffman, E.S., Ono, M., Khanam, D., Hayday, A.C., Frohman, L.A., Koff, A., 1996. Enhanced growth of mice lacking the cyclin-dependent kinase inhibitor function of p27(Kip1). Cell 85, 721–732.

Koff, A., Polyak, K., 1995. p27KIP1, an inhibitor of cyclin-dependent kinases. Prog. Cell Cycle Res. 1, 141–147 [Review] [37 refs].

Lowenheim, H., Furness, D.N., Kil, J., Zinn, C., Gultig, K., Fero, M.L., Frost, D., Gummer, A.W., Roberts, J.M., Rubel, E.W., Hackney, C.M., Zenner, H.P., 1999. Gene disruption of p27(Kip1) allows cell proliferation in the postnatal and adult organ of corti. Proc. Natl. Acad. Sci. USA 96, 4084–4088.

Lumpkin, E.A., Collisson, T., Parab, P., Omer-Abdalla, A., Haeberle, H., Chen, P., Doetzlhofer, A., White, P., Groves, A., Segil, N., Johnson, J.E., 2003. Math1-driven GFP expression in the developing nervous system of transgenic mice. Gene Expr. Patterns 3, 389–395.

Nakayama, K., Ishida, N., Shirane, M., Inomata, A., Inoue, T., Shishido, N., Horii, I., Loh, D.Y., Nakayama, K., 1996. Mice lacking p27(Kip1) display increased body size, multiple organ hyperplasia, retinal dysplasia, and pituitary tumors. Cell 85, 707–720.

Noben-Trauth, K., Zheng, Q.Y., Johnson, K.R., 2003. Association of cadherin 23 with polygenic inheritance and genetic modification of sensorineural hearing loss. Nat. Genet. 35, 21–23.

Raphael, Y., 1993. Reorganization of the chick basilar papilla after acoustic trauma. J. Comp. Neurol. 330, 521–532.

Raphael, Y., Adler, H.J., Wang, Y., Finger, P.A., 1994a. Cell cycle of transdifferentiating supporting cells in the basilar papilla. Hear. Res. 80, 53–63.

Raphael, Y., Athey, B.D., Wang, Y., Lee, M.K., Altschuler, R.A., 1994b. F-actin, tubulin and spectrin in the organ of Corti: comparative distribution in different cell types and mammalian species. Hear. Res. 76, 173–187.

Ruben, R.J., 1967. Development of the inner ear of the mouse: a radio-autographic study of terminal mitoses. Acta Otolaryngol. (Suppl.), 1–44.

Sage, C., Huang, M., Karimi, K., Gutierrez, G., Vollrath, M.A., Zhang, D.S., Garcia-Anoveros, J., Hinds, P.W., Corwin, J.T., Corey, D.P., Chen, Z.Y., 2005. Proliferation of functional hair cells in vivo in the absence of the retinoblastoma protein. Science 307, 1114–1118.

Sasaki, K., Tamura, S., Tachibana, H., Sugita, M., Gao, Y., Furuyama, J., Kakishita, E., Sakai, T., Tamaoki, T., Hashimoto-Tamaoki, T., 2000. Expression and role of p27(kip1) in neuronal differentiation of embryonal carcinoma cells. Brain Res. Mol. Brain Res. 77, 209–221.

Shou, J., Zheng, J.L., Gao, W.Q., 2003. Robust generation of new hair cells in the mature mammalian inner ear by adenoviral expression of Hath1. Mol. Cell. Neurosci. 23, 169–179.

Tarui, T., Takahashi, T., Nowakowski, R.S., Hayes, N.L., Bhide, P.G., Caviness, V.S., 2005. Overexpression of p27Kip1, Probability of Cell Cycle Exit, and Laminar Destination of Neocortical Neurons. Cereb. Cortex. 15, 1343–1355.

Woods, C., Montcouquiol, M., Kelley, M.W., 2004. Math1 regulates development of the sensory epithelium in the mammalian cochlea. Nat. Neurosci. 7, 1310–1318.

ARTICLE IN PRESS

Available online at www.sciencedirect.com
SCIENCE DIRECT®

Hearing Research xxx (2006) xxx–xxx

HEARING RESEARCH

www.elsevier.com/locate/heares

Research paper

Transgene correction maintains normal cochlear structure and function in 6-month-old *Myo15a* mutant mice

Sho Kanzaki [a,b], Lisa Beyer [a], I. Jill Karolyi [c], David F. Dolan [a], Qing Fang [c], Frank J. Probst [c,d], Sally A. Camper [c], Yehoash Raphael [a,*]

[a] *Kresge Hearing Research Institute, University of Michigan, MSRB III Room-9303, Ann Arbor, MI 48109-0648, USA*
[b] *Department of Otolaryngology, Keio University, Shinjuku, Tokyo 160-0016, Japan*
[c] *Department of Human Genetics, University of Michigan, Ann Arbor, MI 48109-0618, USA*
[d] *Department of Molecular and Human Genetics, Baylor College of Medicine, Houston, TX 77030, USA*

Received 18 August 2005; received in revised form 13 January 2006; accepted 30 January 2006

Abstract

The *shaker2* (*sh2*) mouse is a murine model for human non-syndromic deafness *DFNB3*. The mice have abnormal circling behavior suggesting a balanced disorder, and profound deafness. The insertion of a bacterial artificial chromosome (BAC) transgene containing the *Myo15a* gene into *sh2/sh2* zygotes confers hearing capability and abolishes the circling behavior in 1-month-old transgenic animals. In this study, we investigated both the hearing and the morphology of the cochlea in *Myo15a* mutants carrying this BAC transgene at two, four, or six months of age. The hearing threshold of these mice is normal, with no physiologically significant differences compared to age-matched heterozygous *sh2J* mice (with or without the BAC transgene). In six-month-old transgenic mice with the BAC, the morphology of hair cells in the apical and upper basal turns of the cochlea is normal. Hair cells of lower basal turn, however, were missing in some mutant animals. This study demonstrates that BAC transgene correction cannot only maintain normal morphology but also confer stable hearing function in *Myo15a* mutant mice for as long as 6 months. In addition, excess *Myo15a* expression has no physiologically significant protective or deleterious effects on hearing of normal mice, suggesting that the dosage of *Myo15a* may not be problematic for gene therapy.

Keywords: *Shaker2* mouse; Cytocaud; Phenotypic rescue; BAC transgene

1. Introduction

Approximately one half of cases of congenital deafness are thought to be due to genetic causes, and deafness can cause social isolation and developmental problems (Friedman and Griffith, 2003; Morton, 2002). Understanding the molecular and genetic causes of hereditary deafness will help establish better diagnosis and prognosis for deaf patients, and may allow for reversal of hearing loss in the future.

The *shaker2* (*Myo15a*$^{sh2/sh2}$) mouse mutant is deaf and exhibits abnormal circling behavior (Dobrovolskaia-Zavasdkaia, 1928; Probst et al., 1998; Snell and Law, 1939). The mutation has an autosomal recessive mode of transmission, caused by a missense mutation in the *Myo15a* gene on mouse chromosome 11. Mutations in the orthologous human gene cause non-syndromic deafness, *DFNB3* (Liang et al., 1998; Wang et al., 1998). The cochlear phenotype of *Myo15a* mutants is consistent with profound deafness. The stereocilia on both inner and outer hair cells are short and stubby and hair cells eventually degenerate (Deol, 1952). Inner hair cells and vestibular hair cells of *shaker2* mutants exhibit an abnormal tail-like cytoplasmic extension protruding from the basal end of the cell, called the cytocaud

* Corresponding author. Tel.: +1 734 936 9386; fax: +1 734 615 8111.
E-mail address: yoash@umich.edu (Y. Raphael).

0378-5955/$ - see front matter © 2006 Elsevier B.V. All rights reserved.
doi:10.1016/j.heares.2006.01.017

(Anniko et al., 1980; Beyer et al., 2000; Probst et al., 1998). Not all deafness mutations are associated with cytocauds, but they are present in the pirouette mice and the waltzing guinea pig, suggesting that cytocauds may represent a hallmark of a particular type of hair cell developmental failure (Beyer et al., 2000; Kanzaki et al., 2002; Sobin et al., 1982).

Myosin XVa is a motor protein that uses energy from ATP hydrolysis to move along actin filaments. It has a large amino terminal domain with no known function, a typical molecular motor, a neck region with myosin light chain interaction sites, and a large tail region involved in protein localization. Genetic and cell biologic studies have revealed the functional importance of several of these structural domains. The mutation in *shaker2* mice changes a highly conserved amino acid within the motor domain, C1779Y, rendering the protein inactive (Liang et al., 1999; Probst et al., 1998). Another mutant allele of *Myo15a*, *shaker2J*, has a deletion that removes the last 6 exons of the gene, resulting in a protein that lacks a domain thought to be important for interaction with integral membrane proteins (Anderson et al., 2000). There is a region within the Myosin XVa tail that is conserved in several different motor myosin proteins, and mutations in this region cause deafness in humans (Friedman et al., 2002; Liburd et al., 2001). This domain may be involved in protein localization.

Normally Myosin XVa is localized at the tips of hair cell stereocilia (Belyantseva et al., 2003, 2005). It interacts with the PDZ domain of whirlin and is essential for movement of whirlin to the stereociliary tips. Injection of a cDNA encoding the motor, neck and tail regions of Myosin XVa is sufficient to restore the appropriate localization of both Myosin XVa and whirlin in cochlear explants of *shaker2* mice. Thus, interaction between these two proteins is necessary for normal hair cell development and hearing (Belyantseva et al., 2005; Delprat et al., 2005; Mburu et al., 2003).

Probst et al. generated a transgenic *Myo15a*$^{sh2/sh2}$ mouse by insertion of BAC425p24, which contains the *Myo15a* gene (Probst et al., 1998). This transgenic *Myo15a*$^{sh2/sh2}$ animal, named Sebastian, exhibited a Preyer reflex and had no obvious vestibular dysfunction. He was mated with *Myo15a*$^{sh2/sh2}$ females to produce a line. Approximately half of the offspring from these matings could hear. The auditory brain stem responses (ABR) of 4-week-old transgenic mice varied from thresholds of 40–70 dB SPL at 20 kHz (unpublished observations). DNA analysis confirmed that all of the hearing offspring had inherited the BAC425p24 transgene, and all of the deaf offspring did not (Probst et al., 1998). Using light microscopy we determined that the morphology of the transgenic mutant inner ears and stereocilia were normal, and cytocauds were not detected. These data provided proof for the principle that addition of the wild-type gene rescues the phenotype of mice with mutations affecting hearing.

To explore the clinical potential of similar phenotypic rescues, it is necessary to assess the efficacy of transgene correction relative to normal controls. This was not possible in the previous study because there were no normal controls from the same genetic background. It is also necessary to determine whether the correction of inner ear structure and function remain stable in the long term, and evaluate whether there is any deleterious or protective affect of the transgene on hearing in normal mice. In the present study we discovered that the transgene is sufficient for complete phenotypic rescue up to 6 months of age and that it does not alter the hearing of normal mice substantially.

2. Materials and methods

2.1. Animals

The *Myo15a*$^{sh2/sh2}$ mutant, BAC 425p24 transgene-corrected animal was originally generated by pronuclear injection of *Myo15a*$^{sh2/sh2}$ mutant eggs, which are on a mixed genetic background (Probst et al., 1998). The founder male was mated to *Myo15a*$^{sh2/sh2}$ females to produce a line, and the line was banked by cryopreserving embryos generated by mating homozygous *Myo15a* mutant (*Myo15a*$^{sh2/sh2}$) BAC transgene-corrected males to superovulated C57BL6/J females. For the experiments reported here, we thawed the cryopreserved embryos, implanted them in foster females and genotyped the resulting progeny for the presence of the BAC transgene. All progeny were obligate heterozygotes for the *Myo15a*^{sh2} mutation (*sh2*/+). Female progeny that were positive for the BAC transgene were mated to *Myo15a*^{sh2J} mutant males (*sh2*^{J}/*sh2*^{J}), which are on a C57BL/KS-*db m* background (Anderson et al., 2000). Water and standard mouse diet (PMI 5020) were provided ad libitum. Animals were housed in an SPF mouse facility in ventilated cages with automatic watering. The University of Michigan Committee on Use and Care of Animals approved all procedures, and all experiments were conducted in accordance with the principles and procedures outlined in the National Research Council *Guide for the Care and Use of Laboratory Animals.*

2.2. Genotyping

All animals were genotyped by polymerase chain reaction (PCR). PCR amplification and diagnostic restriction digestion detected the presence or absence of the missense mutation in the shaker2 mutant allele of *Myo15a.* PCR amplification detected the junction fragment characteristic of the shaker2J deletion, and of the vector-insert junction fragments used to detect the BAC transgene (Anderson et al., 2000; Liang et al., 1998; Probst et al., 1998).

2.3. Auditory brainstem responses measurement

Animals were anesthetized with a mixture of xylazine (0.00125 mg/kg for mice < 8.0 g and 0.004 mg/kg for mice > 8 g) and ketamine (0.0625 mg/kg for mice < 8 g and 0.12 mg/kg for mice > 8 g) prior to measurement. The animals were placed in a sound-isolated, electrically shielded booth (Acoustic Systems) on a heating pad. Needle elec-

Table 1
Non-Mendelian genotype distribution among progeny of *Myo15a*$^{sh2/+}$, Tg(RP22-425p24)1Sac × *Myo15a*$^{sh2J/sh2J}$ cross

Designation	*Myo15a* genotype	Transgenic	Hearing expected	Progeny observed	% Total
sh2/sh2^{J}BAC+	*sh2/sh2*^{J}	Yes	Yes	63	50
sh2/sh2^{J}BAC−	*sh2/sh2*^{J}	No	No	9	7
sh2^{J}/+BAC+	*sh2*^{J}/+	Yes	Yes	19	15
sh2^{J}/+BAC−	*sh2*^{J}/+	No	Yes	35	28

trodes (Grass E2 platinum) were placed subcutaneously below the tested ear (reference electrode), in the vertex (active electrode), and below the contralateral ear (ground electrode). The sound stimulus consisted of 15 ms tone bursts, (rise-fall time 1 ms) at 4, 10, and 20 kHz. The sound stimuli were delivered into the ear canal from an encased, shielded Beyer earphone through a 13 mm tube. Response waveforms (100,000 gain, filtered from 0.3–3.0 kHz) were averaged (1024 epochs) using a Tucker–Davis data acquisition system. The response threshold was defined as the interpolated value between the last level at which a response was present and 5 dB lower where no response was observed. The sound delivery system was calibrated with a 1/8 in. B&K condenser microphone in a volume approximating the mouse external ear canal and expressed as SPL. ABR tests were performed at 2 months, 4 months, and 6 months of age on 15–17 animals of each of the following three genotypes: *sh2/sh2*^{J}BAC+, *sh2*^{J}/+BAC+ and *sh2*^{J}/+BAC− (see Table 1 and Section 3 for genotypes designations). *sh2/sh2*^{J}BAC− are completely deaf (Beyer et al., 2000; Probst et al., 1998) and were not tested in this set of studies.

2.4. Scanning electron microscopy and transmission electron microscopy

Scanning electron microscopy (SEM) analysis was performed on at least 4 ears of each genotype. Temporal bones were removed, the cochleae exposed and the samples fixed in 2.5% glutaraldehyde in 0.15 M cacodylate buffer. Tissues were processed using the OTOTO method (Osborne et al., 1984). Samples were dehydrated in increasing concentrations of ethanol and critical point dried with CO_2 in a Sam-Dri 790 (Tousmis, Rockville, MD). Samples were examined on a Phillips FEG SEM or an Amray 100B microscope.

Transmission electron microscopy (TEM) analysis was performed on at least 4 ears of each genotype. Tissues were prepared for TEM analysis as previously described (Anderson et al., 2000; Beyer et al., 2000; Raphael et al., 2001).

2.5. Phalloidin staining

Tissues were fixed in 4% paraformaldehyde for 2 h, and then permeabilized with 0.3% Triton X-100 in PBS for 5 min. To label F-actin, tissues were incubated in a rhodamine-conjugated phalloidin diluted 1:100 in PBS for 30 min (Jackson Immunoresearch, West grove, PA). This stain enhances identification of cell types in the sensory epithelium (Raphael et al., 1994) and reveals cytocauds. Tissues were mounted on microscope slides with Crystal/Mount (Biomedia, Foster City, CA). Tissue analysis and epi-fluorescence photomicroscopy were performed on a Leica DMRB microscope with 40× and 100× objective lenses. At least 6 ears from each genotype were processed for phalloidin staining and epi-fluorescence analysis.

3. Results

3.1. Genetic linkage of the BAC transgene and the Myo15a locus

We crossed BAC transgenic mice that were heterozygous for the *sh2* allele with mice homozygous for the *sh2J* allele, i.e., *Myo15*$^{sh2/+}$, Tg (RP22-425p24)1Sac × *Myo15*$^{sh2J/sh2J}$. The resultant progeny were expected to fall into 4 genotype classes. The first genotype carried two different mutant *Myo15a* alleles (*sh2/sh2*^{J}) and the BAC transgene. These *Myo15a* mutant, BAC transgene corrected animals are designated *sh2/sh2*^{J}BAC+, and we expected they would be able to hear. The second genotype carried two different mutant *Myo15a* alleles (*sh2/sh2*^{J}) but did not have the BAC transgene. These mice, designated *sh2/sh2*^{J}BAC−, are expected to demonstrate the typical *Myo15a* mutant phenotype of circling and congenital deafness because compound heterozygotes are affected and phenotypically indistinguishable from mice homozygous for either *sh2* or *sh2J* alleles (Anderson et al., 2000). The third genotype carried only one mutant *Myo15a* allele (*sh2*^{J}/+) and the BAC transgene, designated *sh2*^{J}/+BAC+. Because *sh2*^{J}/+ mice hear normally, these mice should also hear normally, unless MYO15 from the BAC transgene is deleterious. The fourth genotype carried only one mutant *Myo15a* allele (*sh2*^{J}/+) but not the BAC transgene and was designated *sh2*^{J}/+BAC−. The fourth genotype is expected to hear normally.

Myo15a is located centrally on mouse chromosome 11. Transgenes introduced by pronuclear injection integrate randomly at a single genomic site on one of the 20 mouse chromosomes, and then are transmitted stably to progeny in a Mendelian manner. If the BAC integrates on any chromosome other than chromosome 11, then the mutant *sh2* allele of *Myo15a* and the BAC transgene would segregate independently among the experimental progeny, and each of the four genotypes of offspring produced for this experiment would be expected to comprise 25% of the total. However, out of a total of 126 progeny, DNA genotyping detected 50% *sh2/sh2*^{J}BAC+; 7% *sh2/sh2*^{J}BAC−; 15% *sh2*^{J}/BAC+, and 28% in *sh2*^{J}/+BAC− (Table 1). This deviates significantly from the expected distribution ($p = 1.9 \times 10^{-11}$). The BAC frequently co-segregated with the mutant allele of *sh2*, resulting in overrepresentation of *sh2/sh2*^{J}BAC+ progeny and underrepresentation of *sh2/sh2*^{J}BAC− progeny. Thus, the BAC must have integrated on the chromosome carrying the mutant *sh2* allele, i.e., chromosome 11. From these data we cannot distinguish

whether the BAC integration site is located proximal or distal to the *Myo15* locus. Nevertheless, it is clear that the BAC integrated far enough away from *Myo15* that recombination, or crossing over, between the two loci occurs with a frequency sufficient to produce adequate numbers of mice in each genotype class for our study (Snell and Law, 1939).

3.2. Normal hearing in BAC transgenic Myo15a mutant mice

As expected, *sh2/sh2^J*BAC– mice had no Preyer reflex and exhibited circling behavior, but the other three genotypes did have a Preyer reflex and exhibited no obvious behavioral abnormalities. A cohort of mice ($N = 15$–17) in the each of the genotypes (other than the *sh2/sh2^J*BAC– mice) were tested for hearing by ABR at 2, 4 and 6 months of age. There was no significant difference ($p = 0.01$) in hearing between *Myo15a* homozygous mutant transgenic animals and *Myo15a* normal, non-transgenic controls (*sh2/sh2^J*BAC+ versus *sh2^J*/+BAC–) at two months of age at any of the frequencies tested (Fig. 1). Thus, the BAC transgene correction confers the same functional capability as the endogenous wild-type *Myo15a* gene. Similarly, hearing at 4 months of age was generally similar in mice of all three genotypes, at all three frequencies tested. However, approximately 20% of the mice in all three genotypes had elevated thresholds at the 6 months time point at the 20 kHz test. The increase was about 20 dB in these mice and contributed to a small increase in the mean threshold at this frequency as well as larger standard deviations (Fig. 1). The lack of any significant differences among these genotypes suggests that the BAC transgene correction is stable from 2 to 6 months of age. It also appears that the extra dose of *Myo15* provided by the BAC does not confer a significant advantage or disadvantage in heterozygous *Myo15a* mutant mice, although a genetic background with more profound age related hearing loss might be more revealing. Although there are several data points in this study that exhibit differences in hearing thresholds, the differences are within 5 dB and not likely to be significant physiologically. These data contrast with the variability seen in the *sh2/sh2* stock (data not shown), probably due to genetic background differences. The animals in this study are a mixture of C57BL/6J, *sh2* stock and C57BL/KS, and their excellent hearing is likely the result of hybrid vigor.

3.3. Normal actin cytoarchitecture in BAC corrected mutant animals

Phalloidin-stained whole-mounts of the organ of Corti of *sh2^J*/+BAC– mice observed with epi-fluorescence in a focal plane beneath the reticular lamina reveal the borders of inner hair cells where actin is abundant (Fig. 2). A full complement of hair cells was present and their organization in the organ of Corti appeared normal in these heterozygotes (Fig. 2A). In contrast, cochleae of *sh2/sh2^J*BAC– mice contained cytocauds. Cytocauds were prominent in inner hair cells but not in outer hair cells (Fig. 2B). In cochleae obtained from *sh2/sh2^J*BAC+ mice, the organization of stereocilia on hair cells, and the general cytoarchitecture of the organ of Corti appeared normal (Fig. 2C). No cytocauds could be observed in these ears. The organ of Corti in *sh2/sh2^J*BAC+ mice contained all hair cells in the apical

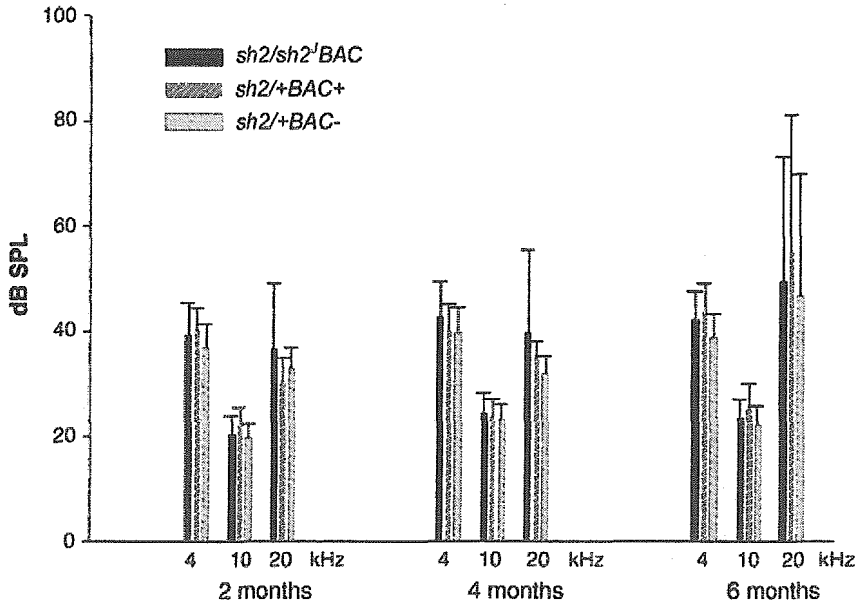

Fig. 1. Stable hearing in aging transgenic mice. ABR thresholds were measured in *sh2/sh2^J*BAC+ transgenic mice (black bars), *sh2*/+BAC+ transgenic mice (red bars), and *sh2*/+BAC– non-transgenic mice (green bars) and reported as average sound pressure level (in dB SPL, with SD) at 4, 10 and 20 kHz. *sh2*/+BAC+ transgenic mice had very slightly higher thresholds than *sh2*/+BAC– non-transgenic mice at a few times and frequencies: 2 months at 4 and 10 kHz ($p = 0.05$), 4 months at 20 kHz ($p = 0.01$), and 6 months at 4 kHz ($p = 0.01$) and 10 kHz ($p = 0.05$). Although the p values reach marginal levels of statistical significance, the fact that the significance is borderline in most cases and that the thresholds vary by less than 10 dB, suggests that an excess dose of *Myo15a* is physiologically inconsequential.

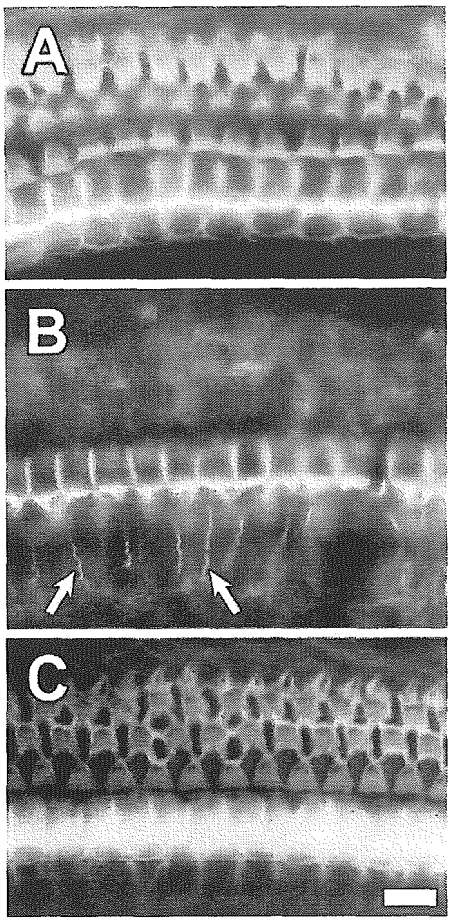

Fig. 2. *sh2/sh2^J*BAC+ mice lack cytocauds. Rhodamine phalloidin staining reveals actin-rich structures in *sh2^J*/+BAC− (A), *sh2/sh2^J*BAC− mutant (B), and *sh2/sh2^J*BAC+ mice (C) at 6 months of age. (A) The junctions between inner and outer hair cells and their supporting cells appear normal and reveal a normal cell complement and organization at the apical surface of the auditory epithelium. (B) Cytocauds (arrows) are prominent at the basal region of nearly every inner hair cell of the *sh2/sh2^J*BAC− mutant mice. Outer hair cells are no longer present at this age. (C) The transgene restores the appearance of the apical surface to that of normal mice (compare to A). No cytocauds are seen at this age. Scale bar = 10 μm.

turn (Fig. 2C) and most hair cells in the upper basal turn (data not shown). The organization of the organ of Corti and the stereocilia on the inner hair cells appeared normal.

3.4. Normal stereocilia on the apical surface of hair cells in mutant transgenic mice

At two months of age most hair cells survived in the apical turn of *sh2/sh2^J*BAC− cochleae (Fig. 3A). These hair cells had short and stubby stereocilia, as seen in previous studies (Anderson et al., 2000; Probst et al., 1998). In the basal cochlear turn, outer hair cells were missing, replaced by phalangeal scars (Fig. 3B). In *sh2^J*/+BAC+ animals, the apical hair cells appeared normal and normally-organized and none appeared to be missing (Fig. 3C). Basal coil hair cells were also present (Fig. 3D), exhibiting a normal surface morphology, suggesting that addition of the BAC to the normal heterozygous mouse does not induce a pathologic change. In *sh2/sh2^J*BAC+ animals, hair cells appeared normal. There was a full complement of hair cells in the apical (Fig. 3E) and mid-basal cochlear turns (Fig. 3F).

3.5. Normal surface appearance in 6-month-old sh2/sh2^{J}BAC+ mice

Six-month-old *sh2/sh2^J*BAC+ animals had a full complement of hair cells in the apical turn and upper basal turn (Fig. 4A and B, respectively), and the cells appeared normal. In the lower basal turn, near the hook, many outer hair cells and some inner hair cells were missing, suggesting ongoing degeneration in this area (Fig. 4C). Loss of hair cells in the extreme basal end of the cochlear duct was also detected in the heterozygotes and wild-type animals analyzed in this study (data not shown). Supporting cells appeared to be present, and the cell surface contour in area of hair cell loss contained typical structure of phalangeal scars (Fig. 4C) resembling scarring seen in the organ of Corti after noise or drug insults. These data suggest that the *Myo15a* mutation does not influence supporting cells and their ability to construct phalangeal scars.

3.6. Normal ultrastructure in 6-month-old sh2/sh2^{J}BAC+ mice

Transmission electron microscope analysis of *sh2/sh2^J*BAC+ cochleae revealed normal morphology of inner hair cells (Fig. 5). Sectioning through entire inner hair cells revealed no cytocauds, in agreement with observation of phalloidin-stained material (Fig. 2C). Stereocilia, cytoplasm and nucleus all had normal appearance. Afferent nerve endings were seen on the membrane of the inner hair cell.

4. Discussion

We have demonstrated that BAC transgene correction with wild-type *Myo15a* corrects structure and function of the inner ear in *sh2/sh2^J* mice and that the phenotypic rescue is stable for at least 6 months. Addition of the BAC transgene leads to expression of the wild-type gene, which avails the wild-type myosin XVa to the cell machinery. The mutated myosin XVa is also present in these animals, indicating that the addition of the normal protein is sufficient for obtaining a phenotypic rescue in this recessive mutation. Correction of dominant mutations is challenging if there is a mutant protein that interferes with the function of normal proteins. In such cases, it may be possible to block expression of the mutated gene or production of the mutated protein with methods such as siRNA. This approach has recently been shown to rescue the phenotype of a dominant negative *GJB2* (connexin 26) mutation (Maeda et al., 2005).

In our study, there was slight variability in the outcome of *Myo15* transgene correction over time, with approxi-

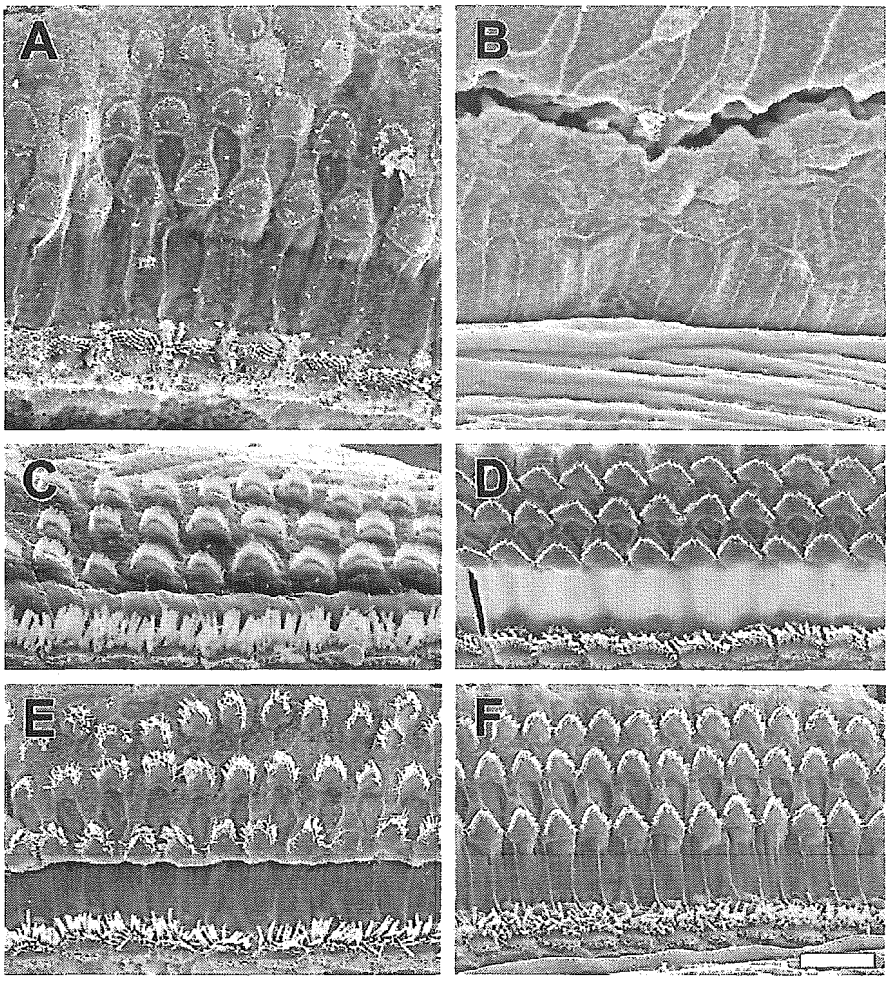

Fig. 3. *sh2/sh2^J*BAC+ mice have normal stereocilia. Scanning electron micrographs of the organ of Corti in apical (A, C, E) and basal (B, D, F) cochlear turns of 2-month-old *sh2/sh2^J*BAC− mutant mouse (A and B), *sh2^J*/+BAC+ (C and D), and *sh2/sh2^J*BAC+ (E and F). (A) A row of inner hair cells and three rows of outer hair cells with no missing hair cells are seen in normal organization, but the stereocilia in all hair cells are very short and stubby. (B) No hair cells are found. (C–F) A full complement of inner and outer hair cells is found and the length and organization of stereocilia appear normal. Scale bar = 10 μm.

mately 20% of the animals in each of the phenotypes demonstrating partial hearing loss at the 6 months time point. Since this variability was seen in wild-type animals with and without the BAC insertion, we speculate that factors other than the mutation cause deterioration of hearing in mice on this genetic background. Aging is probably an important factor in the loss of hair cells and elevation of thresholds in some of these animals. The possible involvement of modifier genes and aging on the long term fate of hair cells and hearing has been demonstrated in other strains (Haider et al., 2002). Because the *sh2* mutation arose on an undefined background, the contribution of the background to the manifestation of the mutation cannot be clearly assessed.

The stability of the correction over several months in the majority of the animals suggests that insertion of the wild-type gene for clinical use may lead to significant and long-term phenotypic rescue. This is important, because recent data show that actin (and probably other proteins) in stereocilia continue recycling after stereocilia are formed (Schneider et al., 2002), suggesting that myosin XVa role in protein transport is important throughout life.

Addition of the BAC to phenotypically normal heterozygotes (*sh2^J*/+BAC+) did not significantly alter their hearing. It is important that there is no deleterious effect despite the expression of the normal gene and the presence of transgenic myosin XVa in the ear and elsewhere (Karolyi et al., 2003). Transgene expression level can vary significantly as a function of the copy number of the integrated transgene and/or the influence of the surrounding DNA. Thus, gene therapy could produce more *Myo15a* than the wild-type allele. In some cases, excess dosage of the normal gene can be deleterious, and cause defects that are as profound as those produced by protein deficiency (FitzPatrick, 2005; Schedl et al., 1996; Yu et al., 1998). Our results indicate that excess myosin XVa does not induce defects.

To design clinically applicable therapies using insertion of wild-type genes, it will be necessary to find ways to

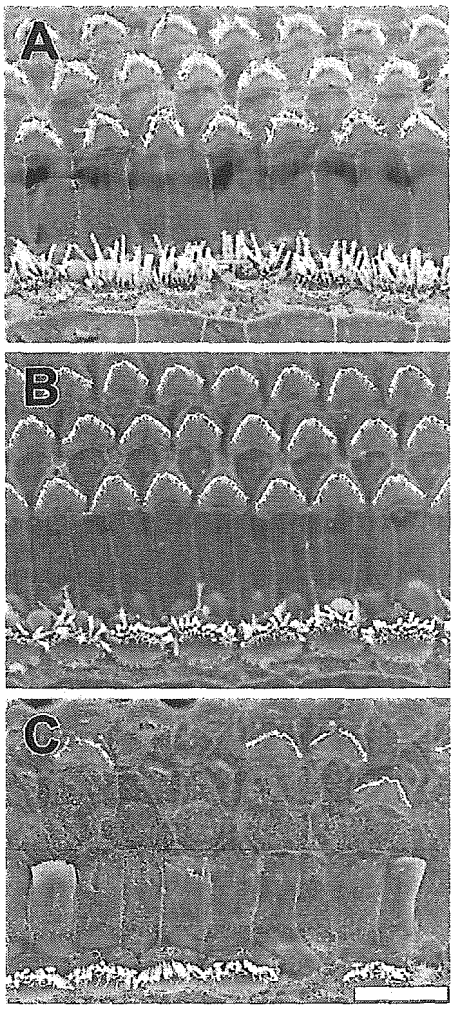

Fig. 4. Partial hair cell loss in *sh2/sh2^J*BAC− mice at the extreme base of the organ of Corti. SEM micrographs of the surface of the organ of Corti in 6-month-old *sh2/sh2^J*BAC+ animals. (A) In the apical turn, no hair cell loss is seen and the size and organization of the stereocilia appears normal. (B) In the upper-basal turn the surface of the organ of Corti appears normal. (C) In the lower basal turn some inner and many outer hair cells are missing. Pillar cells remain in the tissue and the scars appear typical of phalangeal scars of the organ of Corti. Scale bar = 10 μm.

introduce the genes at the optimal time. In the case of recessive mutations, where the pathology is usually congenital, early post-natal treatment will be necessary, and may succeed if hair cells are still available at this time point. However, dominant negative mutations with late onset pathology may be good candidates for phenotypic rescue, by silencing the mutated gene, as recently shown in mice (Maeda et al., 2005).

The finding of outer hair cell loss in the extreme basal end of the cochlear duct was similar in all genotypes studied and coincided with ABR data showing increased thresholds in the high frequencies. We therefore do not attribute this to incomplete phenotypic rescue at the basal cochlear coil. Rather, we conclude that these changes represent first signs of aging in the cochlea. It is unclear why the basal coil is especially susceptible to aging and other types

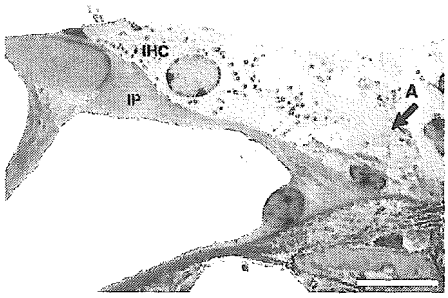

Fig. 5. Normal ultrastructure and innervation of inner hair cells in *Myo15a* mutant transgenic mice. A TEM micrograph showing an inner hair cell of *sh2/sh2^J*BAC+ mouse. No cytocaud is observed. Stereocilia extend from the apical cell surface into the lumen. The inner hair cell appears to have a normal size, and its cytoplasm and nucleus have a normal appearance. An afferent nerve (A) appears to synapse with the hair cell. Scale bar = 10 μm.

of cochlear insults (Keithley and Feldman, 1982; Ohlemiller et al., 2000). We speculate that the higher metabolic activity in the cochlear base (Niedzielski and Schacht, 1991) requires rapid recycling of proteins and remodeling of stereocilia structure in this area, thereby increasing the effects of deficient synthesis of myosin XVa or others proteins.

Transgenic mice with BAC inserts may provide further insight into the role of *Myo15a* in normal hearing. Myosin XVa localizes at the tips of stereocilia with whirlin in normal mice, but both proteins are absent from the tips in *Myo15a$^{sh2/sh2}$* animals, indicating that MYO15A is necessary for transportation of whirlin (Belyantseva et al., 2005). Inducible transgenes could be used to determine whether the presence of MYO15A is necessary during development, when stereocilia extend and attain their normal organization, or whether it is constantly in demand for turnover and recycling of stereocilia proteins.

In conclusion, we demonstrate that BAC transgene insertion in *Myo15a* mutant mice leads to stable structural and functional phenotypic rescue. The phenotypic rescue is stable at least until the age of 6 months. Addition of the BAC transgene into normal heterozygotes does not induce any detectable changes in inner ear structure and function, suggesting that excess *Myo15a* has no significant deleterious effects.

Acknowledgements

The authors thank Gary Dootz, Laura Grant, Karin Halsey, Galina Gavrilina, Merle Rosenzweig and Donald Swiderski for technical assistance. This work was supported by B. and A. Hirschfield, the CHD, GM and the UAW, and NIH NIDCD Grants R01-DC05053, R01-DC01634 and P30 DC05188.

References

Anderson, D.W., Probst, F.J., Belyantseva, I.A., Fridell, R.A., Beyer, L., Martin, D.M., Wu, D., Kachar, B., Friedman, T.B., Raphael, Y.,